Orbital angular momentum density and spiral spectra of Lorentz–Gauss vortex beams passing through a single slit*

Zhi-Yue Ji(季志跃) and Guo-Quan Zhou(周国泉)†

School of Sciences, Zhejiang A & F University, Lin'an 311300, *China*

(Received 24 March 2017; revised manuscript received 19 April 2017; published online 18 July 2017)

Based on the Hermite–Gaussian expansion of the Lorentz distribution and the complex Gaussian expansion of the aperture function, an analytical expression of the Lorentz–Gauss vortex beam with one topological charge passing through a single slit is derived. By using the obtained analytical expressions, the properties of the Lorentz–Gauss vortex beam passing through a single slit are numerically demonstrated. According to the intensity distribution or the phase distribution of the Lorentz–Gauss vortex beam, one can judge whether the topological charge is positive or negative. The effects of the topological charge and three beam parameters on the orbital angular momentum density as well as the spiral spectra are systematically investigated respectively. The optimal choice for measuring the topological charge of the diffracted Lorentz–Gauss vortex beam is to make the single slit width wider than the waist of the Gaussian part.

Keywords: Lorentz–Gauss vortex beam, single slit, orbital angular momentum density, topological charge

PACS: 42.25.Fx, 42.50.Tx, 42.60.Jf, 42.79.Ag **DOI:** 10.1088/1674-1056/26/9/094202

1. Introduction

The spreading of the Lorentzian distribution is proved to be higher than that of the Gaussian one.[1–4] Therefore, the combination of Lorentzian and Gaussian distributions, namely, the Lorentz–Gauss beam, can be used to describe the radiation emitted by a single mode laser diode.[5,6] The Lorentz–Gauss beam is the lowest–order mode of a super–Lorentz–Gauss beam family.[7,8] The properties of Lorentz–Gauss beams, including the beam propagation factor,[9] the focal shift,[10] the Wigner distribution,[11] the tight focusing,[12] and the radiation force,[13] have been extensively investigated. Also, the propagation of Lorentz–Gauss beams has been widely examined in various media such as free space,[2,14] a turbulent atmosphere,[15] a uniaxial crystal,[16,17] a Kerr medium,[18] and a strongly nonlocal nonlinear medium.[19]

When the radiation emitted by a single mode diode laser goes through a spiral phase plate, the output is called the Lorentz–Gauss vortex beam. Its properties including the beam propagation factor, the kurtosis parameter, the focusing, the tunable optical gradient force, and the Wigner distribution have been studied.[20–25] Propagations of Lorentz–Gauss vortex beams in free space, in a turbulent atmosphere, and in a uniaxial crystal have also been demonstrated.[26–28] However, the major advantage of a Lorentz–Gauss vortex beam is that it carries the orbital angular momentum. In other words, the Lorentz–Gauss vortex beam carries a topological charge. Therefore, one tends to focus on the study of the topological charge or the orbital angular momentum of the Lorentz–Gauss vortex beam. The pioneering work reported the orbital angular momentum density of a general Lorentz–Gauss vortex beam in free space.[29] Nevertheless, a more effective method to measure the orbital angular momentum is the diffraction of the vortex beam by an obstacle.[30–34] The typical and simplest obstacle is the single slit. In the remainder of this paper, the diffraction of the Lorentz–Gauss vortex beam by a single slit is studied.

2. Orbital angular momentum density and spiral spectra of Lorentz–Gauss vortex beams passing through a single slit

In the Cartesian coordinate system, the z axis is taken to be the propagation axis. The single slit is located at the x axis as shown in Fig. 1. The width of the single slit is a. The incident optical beam is a Lorentz–Gauss vortex beam, which is described by

$$\begin{bmatrix} E_{+1}(x_0,y_0,0) \\ E_{-1}(x_0,y_0,0) \end{bmatrix} = \frac{w_{0x}w_{0y}}{(w_{0x}^2+x_0^2)(w_{0y}^2+y_0^2)} \exp\left(-\frac{x_0^2+y_0^2}{w_0^2}\right) \begin{bmatrix} x_0+\mathrm{i}y_0 \\ x_0-\mathrm{i}y_0 \end{bmatrix}, \quad (1)$$

where w_0 is the waist of the Gaussian part, and w_{0x} and w_{0y} are the width parameters of the Lorentzian part in the x and y directions, respectively. Here, the Lorentz–Gauss vortex beam carries one topological charge. $E_{+1}(x_0,y_0,0)$ denotes that the topological charge is 1. $E_{-1}(x_0,y_0,0)$ means that the topological charge is -1. The Lorentz–Gauss vortex beam passing through the single slit obeys the well known Collins integral

*Project supported by the National Natural Science Foundation of China (Grant No. 11574272) and Zhejiang Provincial Natural Science Foundation of China (Grant No. LY16A040014).

†Corresponding author. E-mail: zhouguoquan178@sohu.com

© 2017 Chinese Physical Society and IOP Publishing Ltd

formula[35]

$$E_M(x,y,z) = \frac{1}{\mathrm{i}\lambda z}\exp(\mathrm{i}kz)\int_{-\infty}^{\infty}\int_{-a/2}^{a/2} E_M(x_0,y_0,0) \times \exp\left\{\frac{\mathrm{i}k}{2z}[(x-x_0)^2+(y-y_0)^2]\right\}\mathrm{d}x_0\,\mathrm{d}y_0, \quad (2)$$

where $k = 2\pi/\lambda$ is the wave number, λ is the optical wavelength in free space, and M is the topological charge. To obtain the analytical expression of $E_M(x,y,z)$, the Lorentz distribution should be expanded into the linear superposition of Hermite–Gaussian functions[36]

$$\frac{1}{w_{0x}^2+x_0^2} = \frac{\sqrt{\pi}}{\sqrt{2}w_{0x}^2}\sum_{m=0}^{N}\sigma_{2m}H_{2m}\left(\frac{x_0}{w_{0x}}\right)\exp\left(-\frac{x_0^2}{2w_{0x}^2}\right), \quad (3)$$

where N is the term number of the expansion, and H_{2m} is the $2m$-th order Hermite polynomial. The expanded coefficient σ_{2m} is given by[36]

$$\sigma_{2m} = \frac{(-1)^m\sqrt{2}}{2^{2m}}\left\{\frac{1}{m!}\mathrm{erfc}\left(\frac{\sqrt{2}}{2}\right)\exp\left(\frac{1}{2}\right) + \sum_{n_1=1}^{m}\frac{2^{2n_1}}{(2n_1)!(m-n_1)!}\left[\left\{\mathrm{erfc}\left(\frac{\sqrt{2}}{2}\right)\exp\left(\frac{1}{2}\right) + \sqrt{\frac{2}{\pi}}\sum_{n_2=1}^{n_1}(-1)^{n_2}(2n_2-3)!!\right]\right\}, \quad (4)$$

where erfc is the complementary error function. The value of σ_{2m} dramatically decreases with increasing even number $2m$. Here $\sigma_0 = 0.7399$, $\sigma_2 = 0.9298\times10^{-2}$, and $\sigma_6 = 1.112\times10^{-4}$. Then we introduce the aperture function $\mathrm{circ}(\zeta)$, which is defined by

$$\mathrm{circ}(\zeta) = \begin{cases} 1, & 0 \le \zeta < 1, \\ 0, & \zeta \ge 1. \end{cases} \quad (5)$$

Moreover, the aperture function is expanded as a finite sum of complex Gaussian functions

$$\mathrm{circ}(\zeta) = \sum_{l=1}^{15}\alpha_l\exp(-\beta_l\zeta^2), \quad \zeta\in[0,\infty), \quad (6)$$

where the complex expanded and the Gaussian coefficients α_l and β_l could be obtained by the optimization computation.[37] The expansion of the aperture function into 15 terms of complex Gaussian functions is shown in Fig. 2. The dotted curve in Fig. 2 is added to demonstrate Eq. (5). Only at the edge of the aperture, the difference between Eqs. (5) and (6) is apparent.

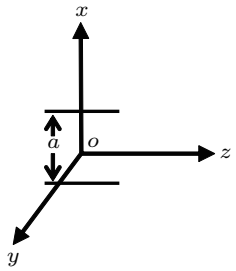


Fig. 1. The single slit in the Cartesian coordinate system.

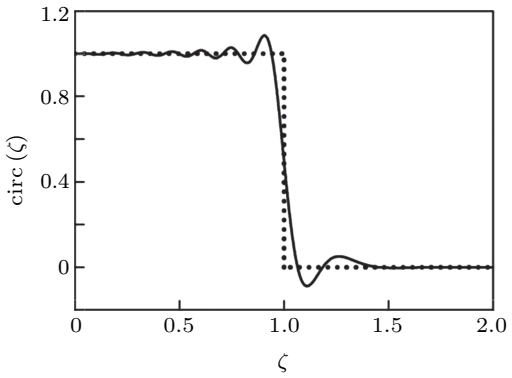


Fig. 2. The expansion of the aperture function into 15 terms of complex Gaussian functions.

Finally, the following mathematical formulae are used:[38]

$$H_{2m}(x) = \sum_{s=0}^{m}\frac{(-1)^s(2m)!}{s!(2m-2s)!}(2x)^{2m-2s}, \quad (7)$$

$$\int_{-\infty}^{\infty}x^p\exp(-bx^2+2cx)\mathrm{d}x = p!\sqrt{\frac{\pi}{b}}\left(\frac{c}{b}\right)^p\exp\left(\frac{c^2}{b}\right)\sum_{u=0}^{[p/2]}\frac{1}{u!(N-2u)!}\left(\frac{b}{4c^2}\right)^u, \quad (8)$$

where $[p/2]$ gives the greatest integer less than or equal to $p/2$. After the above operations, the analytical expression of the Lorentz–Gauss vortex beam passing through a single slit reads

$$\begin{bmatrix} E_{+1}(x,y,z) \\ E_{-1}(x,y,z)\end{bmatrix} = \frac{1}{\mathrm{i}\lambda z}\exp(\mathrm{i}kz)\begin{bmatrix} T_1(x,z;1)T_2(y,z;0)+\mathrm{i}T_1(x,z;0)T_2(y,z;1) \\ T_1(x,z;1)T_2(y,z;0)-\mathrm{i}T_1(x,z;0)T_2(y,z;1)\end{bmatrix}, \quad (9)$$

with $T_1(x,z;v)$ and $T_2(y,z;v)$ being given by

$$T_1(x,z;v) = \frac{\pi}{\sqrt{2}w_{0x}}\exp\left(\frac{\mathrm{i}kx^2}{2z}\right)\sum_{l=1}^{15}\sum_{m=0}^{N}\sum_{s=0}^{m}\frac{(-1)^s\alpha_l\sigma_{2m}(2m)!a^{2m-2s+v+1}(2m-2s+v)!}{s!(2m-2s)!2^v w_{0x}^{2m-2s}\sqrt{\eta_l}}\left(-\frac{\mathrm{i}kax}{4\eta_l z}\right)^{2m-2s+v} \times\exp\left(-\frac{k^2a^2x^2}{16\eta_l z^2}\right)\sum_{u=0}^{[(2m-2s+v)/2]}\frac{1}{u!(2m-2s+v-2u)!}\left(-\frac{4\eta_l z^2}{k^2a^2x^2}\right)^u, \quad (10)$$

$$T_2(y,z;v) = \frac{\pi}{\sqrt{2b_2}w_{0y}}\exp\left(-\frac{k^2y^2}{4b_2z^2}+\frac{\mathrm{i}ky^2}{2z}\right)\sum_{m=0}^{N}\sum_{s=0}^{m}\frac{(-1)^s\sigma_{2m}(2m)!2^{2m-2s}(2m-2s+v)!}{s!(2m-2s)!w_{0y}^{2m-2s}}$$
$$\times\left(-\frac{\mathrm{i}ky}{2b_2z}\right)^{2m-2s+v}\sum_{u=0}^{[(2m-2s+v)/2]}\frac{1}{u!(2m-2s+v-2u)!}\left(-\frac{b_2z^2}{k^2y^2}\right)^u, \tag{11}$$

where the auxiliary parameters η_l and b_2 are defined as follows:

$$\eta_l = \beta_l + \left(\frac{1}{w_0^2}+\frac{1}{2w_{0x}^2}-\frac{\mathrm{i}k}{2z}\right)\frac{a^2}{4}, \tag{12}$$

$$b_2 = \frac{1}{w_0^2}+\frac{1}{2w_{0y}^2}-\frac{\mathrm{i}k}{2z}. \tag{13}$$

The intensity distribution and the phase distribution of the Lorentz–Gauss vortex beam passing through a single slit turn out to be

$$I_M(x,y,z) = |E_M(x,y,z)|^2, \tag{14}$$

$$\varphi_M(x,y,z) = \mathrm{Arg}[E_M(x,y,z)]. \tag{15}$$

The orbital angular momentum density of the Lorentz–Gauss vortex beam passing through a single slit is given by[39]

$$J_z = \frac{\mathrm{i}\varepsilon_0}{\omega}\left\{x\left[E_M^*(x,y,z)\frac{\partial E_M(x,y,z)}{\partial y} - E_M(x,y,z)\frac{\partial E_M^*(x,y,z)}{\partial y}\right]\right.$$
$$\left. - y\left[E_M^*(x,y,z)\frac{\partial E_M(x,y,z)}{\partial x} - E_M(x,y,z)\frac{\partial E_M^*(x,y,z)}{\partial x}\right]\right\}, \tag{16}$$

where ω is the circular frequency. ε_0 is the electric permittivity of a vacuum, and the asterisk denotes the complex conjugation. To obtain the spiral spectra of the Lorentz–Gauss vortex beam through a single slit, x and y in Eq. (9) are replaced by $\rho\cos\theta$ and $\rho\sin\theta$, respectively. Thus, one has

$$\begin{bmatrix}E_{+1}(\rho,\theta,z)\\E_{-1}(\rho,\theta,z)\end{bmatrix} = \begin{bmatrix}E_{+1}(x,y,z)\\E_{-1}(x,y,z)\end{bmatrix}. \tag{17}$$

Then, the optical field of the Lorentz–Gauss vortex beam passing through a single slit can be expanded as[40]

$$E_M(\rho,\theta,z) = \frac{1}{\sqrt{2\pi}}\sum_{n=-\infty}^{\infty}a_n(\rho,z)\exp(\mathrm{i}n\theta), \tag{18}$$

where a_n is given by

$$a_n(\rho,z) = \frac{1}{\sqrt{2\pi}}\int_0^{2\pi}E_M(\rho,\theta,z)\exp(-\mathrm{i}n\theta)\,\mathrm{d}\theta. \tag{19}$$

The total power of the Lorentz–Gauss vortex beam passing through a single slit yields

$$C = \sum_n C_n, \tag{20}$$

where C_n reads

$$C_n = \int_0^{\infty}|a_n(\rho,z)|^2\rho\,\mathrm{d}\rho. \tag{21}$$

The weight coefficient of each spiral spectrum for the Lorentz–Gauss vortex beam passing through a single slit can be calculated by

$$P_n = \frac{C_n}{C}. \tag{22}$$

3. Numerical calculations and analyses

According to the obtained analytical expressions, the properties of the Lorentz–Gauss vortex beam passing through a single slit are numerically demonstrated. The calculation parameters are set as follows: $\lambda = 0.8$ μm, $a = 1$ mm, and $z = 0.5$ m. Figures 3 and 4 represent the normalized intensity and the phase distributions of the diffracted Lorentz–Gauss vortex beam with $w_0 = w_{0x} = w_{0y} = 1$ mm, respectively. When the topological charge is equal to zero, the expansion of the beam spot in the y direction is larger than that in the x direction

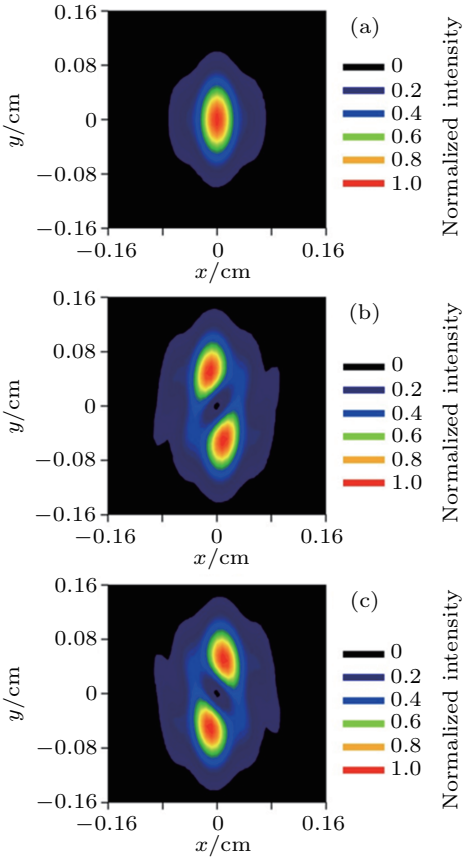


Fig. 3. (color online) The normalized intensity distribution of the diffracted Lorentz–Gauss vortex beam: (a) $M = 0$, (b) $M = 1$, (c) $M = -1$.

due to the confinement of the single slit. When the topological charge is equal to 1, the beam spot is composed of two lobes. Moreover, the orientation of the upper lobe is close to the left, and that of the lower lobe is close to the right. However, when the topological charge is equal to -1, the positions of the two lobes are just the opposite. That is, the upper lobe is located close to the right and the lower lobe is near the left. Figure 4 shows that the phase in the central region is symmetrical when the topological charge is equal to zero. When the topological charge is equal to 1, the phase in the upper central region is positive and that in the lower central region is negative. When the topological charge is equal to -1, the phase is negative in the upper central region and positive in the lower central region. The normalized intensity distribution in the case of $M = 1$ is x-axial symmetrical to that of $M = -1$. So are the phase distributions in the cases of $M = 1$ and $M = -1$.

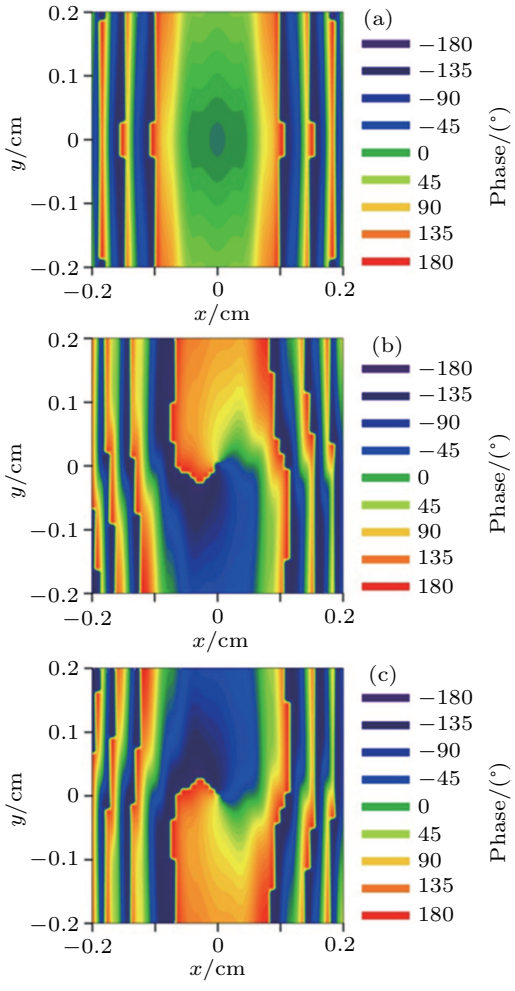


Fig. 4. (color online) The phase distribution of the diffracted Lorentz–Gauss vortex beam: (a) $M = 0$, (b) $M = 1$, (c) $M = -1$.

Here we mainly focus on the effects of the topological charge and three beam parameters on the orbital angular momentum density and the spiral spectra. The orbital angular momentum density distribution of the diffracted Lorentz–Gauss vortex beam with $w_0 = w_{0x} = w_{0y} = 1$ mm is shown in Fig. 5. When the topological charge is equal to zero, the orbital angular momentum density is positive in the first and the third quadrants and negative in the second and the fourth quadrants. Moreover, the area of the orbital angular momentum density in each quadrant is equivalent. Therefore, the overall orbital angular momentum is zero. The orbital angular momentum density distribution contains many lobes when the topological charge is 1 and -1. The magnitude of the negative orbital angular momentum density is far larger than that of the positive orbital angular momentum density when the topological charge is 1. Accordingly, the overall orbital angular momentum is negative, which only indicates the spiral direction. When the topological charge is -1, however, the magnitude of the positive orbital angular momentum density is far larger than that of the negative orbital angular momentum density, resulting in the positive overall orbital angular momentum. The influence of the parameter w_{0x} on the orbital angular momentum density distribution of the diffracted Lorentz–Gauss vortex beam is plotted in Fig. 6, where $w_0 = w_{0y} = 1$ mm and $M = 1$. With decreasing parameter w_{0x}, the magnitude of the orbital angular momentum density increases but the

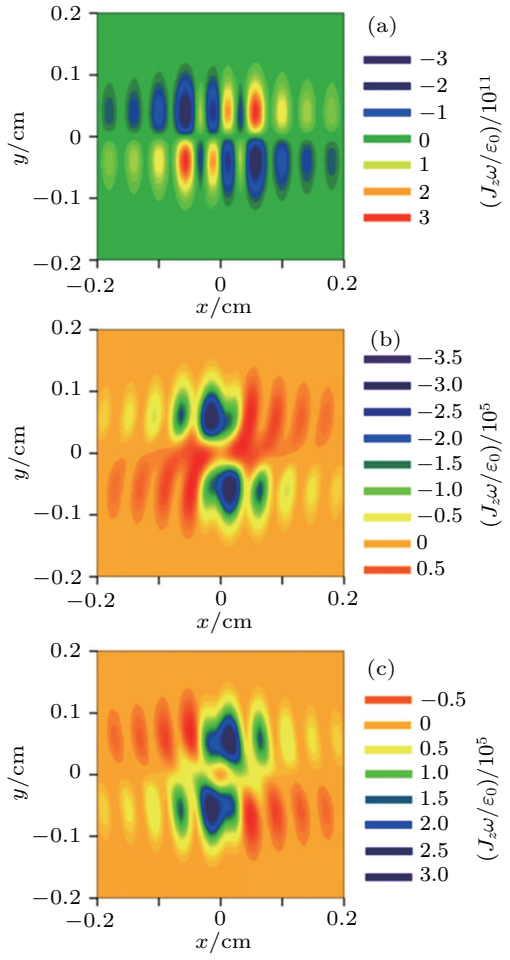


Fig. 5. (color online) The orbital angular momentum density distribution of the diffracted Lorentz–Gauss vortex beam with $w_0 = w_{0x} = w_{0y} = 1$ mm: (a) $M = 0$, (b) $M = 1$, (c) $M = -1$.

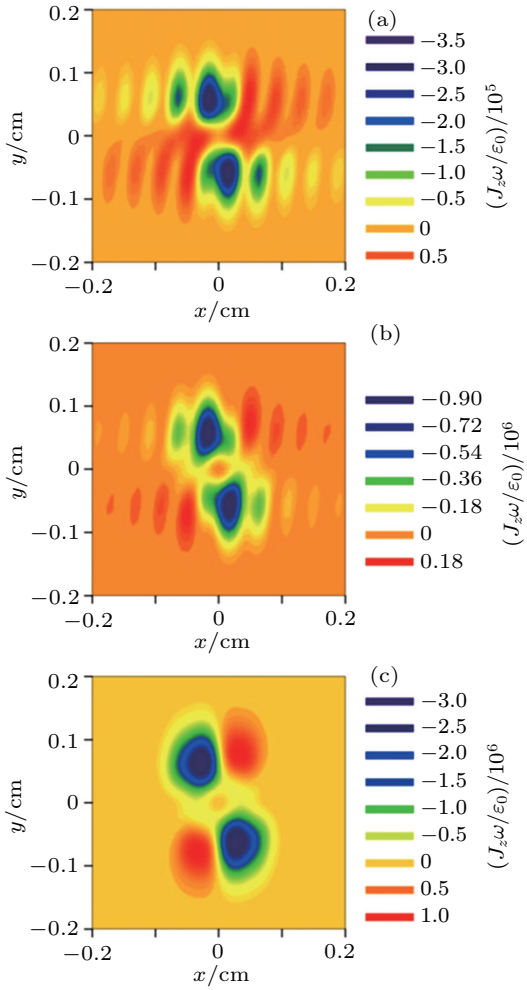


Fig. 6. (color online) The orbital angular momentum density distribution of the diffracted Lorentz–Gauss vortex beam with $w_0 = w_{0y} = 1$, $M = 1$: (a) $w_{0x} = 1$ mm, (b) $w_{0x} = 0.5$ mm, (c) $w_{0x} = 0.2$ mm.

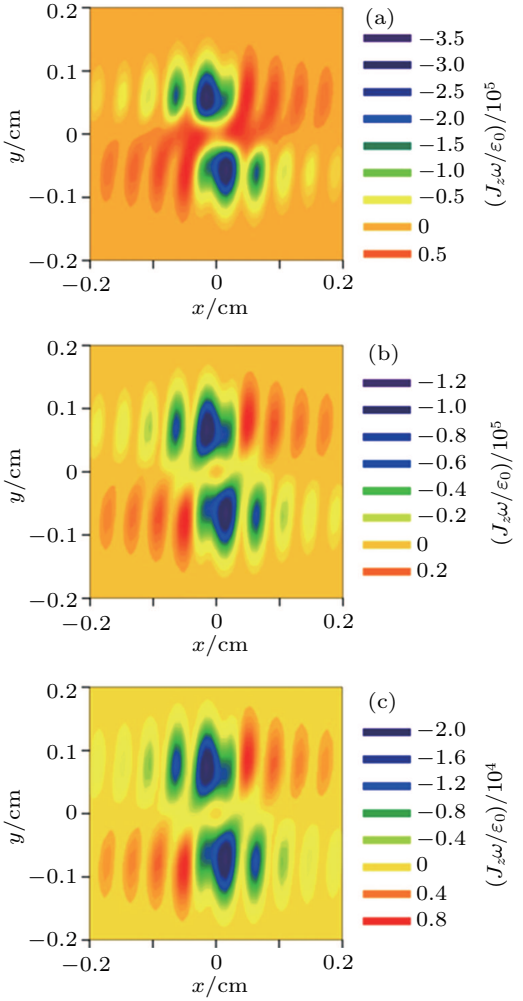


Fig. 7. (color online) The orbital angular momentum density distribution of the diffracted Lorentz–Gauss vortex beam with $w_0 = w_{0x} = 1$ mm, $M = 1$: (a) $w_{0y} = 1$ mm, (b) $w_{0y} = 2$ mm, (c) $w_{0y} = 5$ mm.

number of the lobes decreases. The shape of the orbital angular momentum density distribution also changes with decreasing parameter w_{0x}. The influence of the parameter w_{0y} on the orbital angular momentum density distribution of the diffracted Lorentz–Gauss vortex beam is shown in Fig. 7, where $w_0 = w_{0x} = 1$ mm and $M = 1$. With increasing parameter w_{0y}, the magnitude of the orbital angular momentum density decreases, and the shape of the distribution of the orbital angular momentum density nearly keeps stable. Figure 8 presents the influence of the parameter w_0 on the orbital angular momentum density distribution of the diffracted Lorentz–Gauss vortex beam with $w_{0x} = w_{0y} = 1$ mm and $M = 1$. Both the magnitude and pattern size of the orbital angular momentum density increase with increasing parameter w_0. Among the three beam parameters w_0, w_{0x}, and w_{0y}, the shape of the orbital angular momentum density distribution is most sensitive to the parameter w_0, and the magnitude of the orbital angular momentum density is most insensitive to the parameter w_0.

The influence of the topological charge on the spiral spectra of the diffracted Lorentz–Gauss vortex beam is demonstrated in Fig. 9, where $w_0 = w_{0x} = w_{0y} = 1$ mm. The spiral spectra of the diffracted Lorentz–Gauss vortex beam expand due to the stronger diffraction effect caused by the single slit. When the topological charge is zero, the spectra of $n = 0, \pm 2, \pm 4$, and ± 6 can be observed obviously. The zero-order spectrum is dominant, and the corresponding weight coefficient is close to 0.80. The weight coefficient of $n = \pm 6$ is so small that it can be neglected. When the topological charge is 1, the spectrum of $n = 1$ is dominant and the corresponding weight coefficient is close to 0.72. The spectra of $n = -1$ and 3, $n = -3$ and 5, $n = -5$ and 7, $n = -7$ and 9, $n = -9$ and 11 appear in the spiral spectra of $M = 1$. The weight coefficient of $n = -1$ and 3 is the second largest, and the weight coefficient of $n = -9$ and 11 is very small. The spiral spectra of $M = -1$ are just the parallel shift of the spiral spectra of $M = 1$.

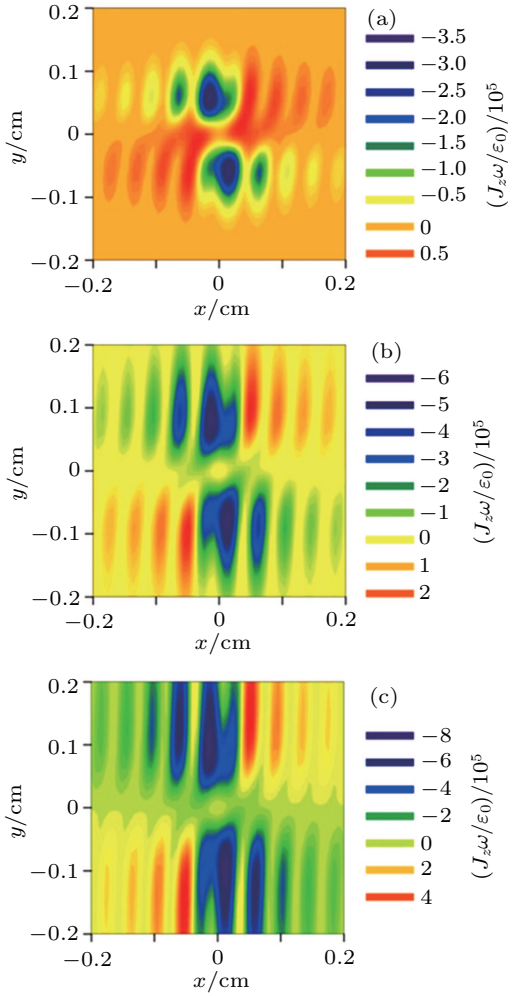


Fig. 8. (color online) The orbital angular momentum density distribution of the diffracted Lorentz–Gauss vortex beam with $w_{0x} = w_{0y} = 1$ mm, $M = 1$: (a) $w_0 = 1$ mm, (b) $w_0 = 2$ mm, (c) $w_0 = 5$ mm.

Figure 10 presents the influence of the beam parameter w_{0x} on the spiral spectra of the diffracted Lorentz–Gauss vortex beam with $w_0 = w_{0y} = 1$ mm and $M = 1$. With decreasing beam parameter w_{0x}, the weight coefficient of the dominant spectrum decreases, but the weight coefficient of the other spectra slowly increases. With decreasing beam parameter w_{0x}, the spiral spectra slightly expand, which indicates that the expansion of the spiral spectra is not very sensitive to the beam parameter w_{0x}. The influence of the beam parameter w_{0y} on the spiral spectra of the diffracted Lorentz–Gauss vortex beam with $w_0 = w_{0x} = 1$ mm and $M = 1$ is shown in Fig. 11. With increasing beam parameter w_{0y}, the weight coefficient of the dominant spectrum decreases, and the weight coefficient of the other spectra increases. With increasing beam parameter w_{0y}, the spiral spectra expand. It is because the reverse change of the parameter w_{0y} in the y direction is similar to the positive change of the parameter w_{0x} in the x direction. Figure 12 shows the influence of the beam parameter w_0 on the spiral spectra of the diffracted Lorentz–Gauss vortex beam with $w_{0x} = w_{0y} = 1$ mm and $M = 1$. Compared with the case of beam parameters w_{0x} and w_{0y}, the weight coefficient of the dominant spectrum decreases much quicker with increasing beam parameter w_0. The weight coefficient of other spectra in Fig. 12(c) can even be detected for $n = 20$. The spiral spectra also expand with increasing beam parameter w_0 due to a stronger diffraction effect. The influence of the parameter w_0 on the spiral spectra is not similar to that of the parameter w_{0x}. This is because the parameter w_{0x} in Eq. (3) appears in both the Hermite polynomial and the Gaussian function.

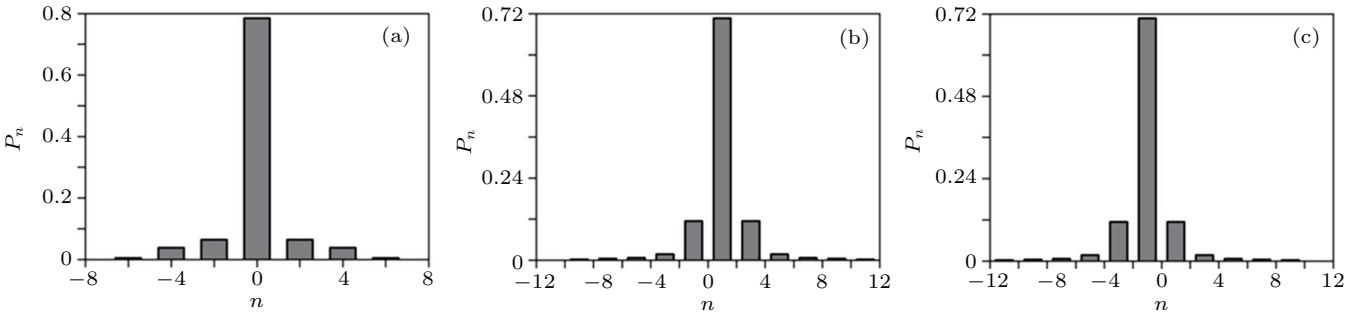


Fig. 9. The influence of the topological charge on the spiral spectra of the diffracted Lorentz–Gauss vortex beam with $w_0 = w_{0x} = w_{0y} = 1$ mm: (a) $M = 0$, (b) $M = 1$, (c) $M = -1$.

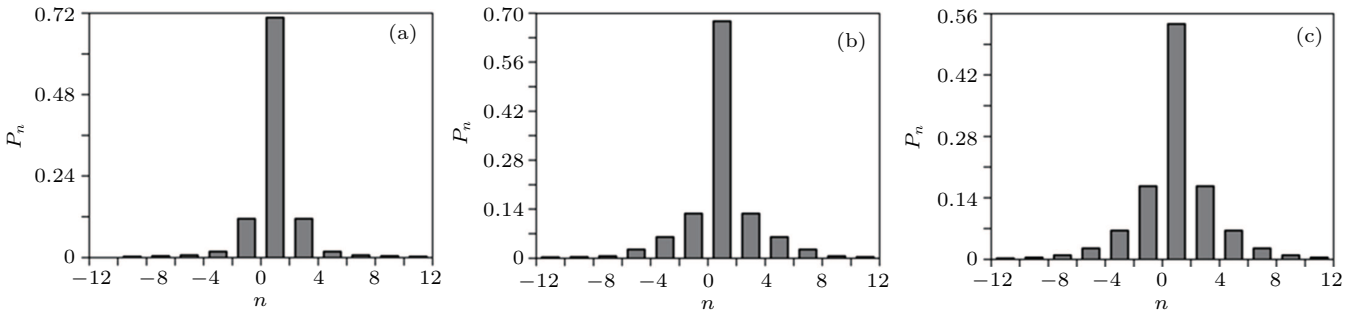


Fig. 10. The influence of the beam parameter w_{0x} on the spiral spectra of the diffracted Lorentz–Gauss vortex beam with $w_0 = w_{0y} = 1$ mm, $M = 1$: (a) $w_{0x} = 1$ mm, (b) $w_{0x} = 0.5$ mm, (c) $w_{0x} = 0.2$ mm.

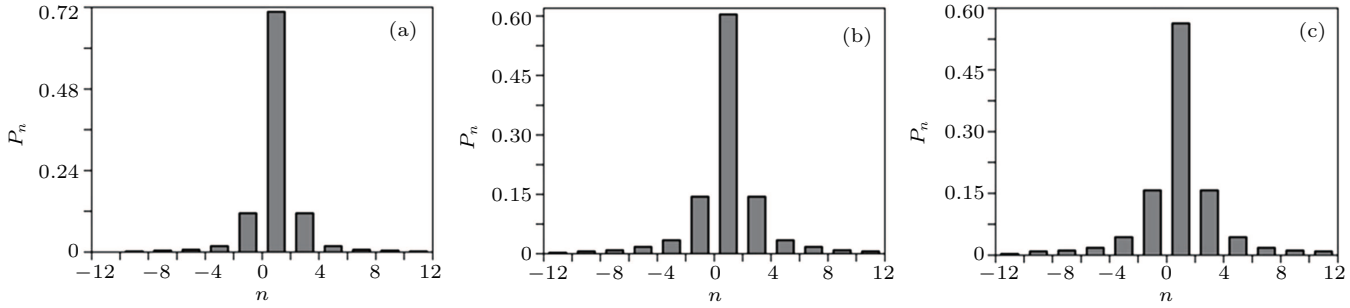


Fig. 11. The influence of the beam parameter w_{0y} on the spiral spectra of the diffracted Lorentz–Gauss vortex beam with $w_0 = w_{0x} =$ 1 mm, $M = 1$: (a) $w_{0y} = 1$ mm, (b) $w_{0y} = 2$ mm, (c) $w_{0y} = 5$ mm.

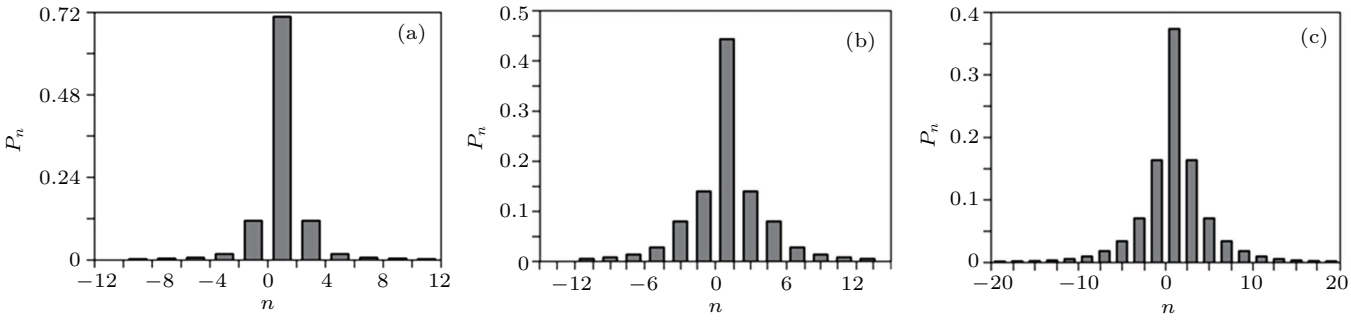


Fig. 12. The influence of the beam parameter w_0 on the spiral spectra of the diffracted Lorentz–Gauss vortex beam with $w_{0x} = w_{0y} =$ 1 mm, $M = 1$: (a) $w_0 = 1$ mm, (b) $w_0 = 2$ mm, (c) $w_0 = 5$ mm.

4. Conclusion

Based on the Hermite–Gaussian expansion of the Lorentz distribution and the complex Gaussian expansion of the aperture function, an analytical expression of the Lorentz–Gauss vortex beam with one topological charge passing through the single slit is derived. Due to these two expansions, the analytical expression is approximate. The normalized intensity and the phase distributions of the diffracted Lorentz–Gauss vortex beam are numerically demonstrated in the reference plane. One can judge whether one topological charge is positive or negative according to the intensity distribution or the phase distribution of the diffracted Lorentz–Gauss vortex beam. The effects of the topological charge and the three beam parameters on the orbital angular momentum density of the diffracted Lorentz–Gauss vortex beam are systematically studied. The sign of the topological charge not only affects the sign of the orbital angular momentum density, but also affects the orientation of the orbital angular momentum density distribution. With decreasing one of the parameters w_{0x} and w_{0y} or increasing the parameter w_0, the magnitude of the orbital angular momentum density increases. The shape of the orbital angular momentum density distribution is most sensitive to the parameter w_0, and the magnitude of the orbital angular momentum density is most insensitive to the parameter w_0. The influences of the three beam parameters on the spiral spectra of the diffracted Lorentz–Gauss vortex beam are also investigated. When the parameter w_0 increases, the diffraction effect becomes stronger. As a result, the spiral spectra of the diffracted Lorentz–Gauss vortex beam expand. As the parameter w_{0x} in Eq. (3) appears in both the Hermite polynomial and the Gaussian function, the influence of the parameter w_{0x} on the spiral spectra is not similar to that of the parameter w_0. The numerical result denotes that the spiral spectra expand slowly with decreasing parameter w_{0x}. It seems that the expansion of the spiral spectra is not very sensitive to the parameter w_{0x}. With increasing parameter w_{0y}, the spiral spectra expand. The reason is that the reverse change of the parameter w_{0y} in the y direction is similar to the positive change of w_{0x} in the x direction. The present study is useful for the measurement of the topological charges of vortex beams. Therefore, the best choice for measuring the topological charge of the diffracted Lorentz–Gauss vortex beam is to make the single slit width larger than the waist of the Gaussian part. The current research is helpful not only to deepen the recognition of the properties of Laguerre–Gaussian beams, but also to the application of the orbital angular momentum.[41–45]

References

[1] Dumke P 1975 *J. Quantum Electron.* **11** 400
[2] Gawhary O E and Severini S 2006 *J. Opt. A: Pure Appl. Opt.* **8** 409
[3] Zhou G Q and Chu X X 2010 *Opt. Laser Technol.* **42** 1093
[4] Zhou G Q 2009 *Opt. Laser Technol.* **41** 953
[5] Naqwi A and Durst F 1990 *Appl. Opt.* **29** 1780
[6] Yang J, Chen T T, Ding G L and Yuan X 2008 *Proc. SPIE* **6824** 68240A
[7] Zhou G Q 2010 *Chin. Phys. B* **19** 064201
[8] Zhou G Q 2011 *Chin. Phys. B* **20** 0114103
[9] Zhou G Q 2009 *Appl. Phys. B* **96** 149
[10] Zhou G Q 2008 *J. Opt. Soc. Am. A* **25** 2594
[11] Torre A 2012 *Appl. Phys. B* **109** 671
[12] Saraswathi R C, Prabakaran K, Rajesh K B and Jaroszewicz Z 2014 *Optik* **125** 5339

[13] Jiang Y F, Huang K K and Lu X H 2011 *Opt. Express* **19** 9708
[14] Zhou G Q 2009 *Acta Phys. Sin.* **58** 6185 (in Chinese)
[15] Zhou G Q and Chu X X 2010 *Opt. Express* **18** 726
[16] Zhao C L and Cai Y J 2010 *J. Mod. Opt.* **57** 375
[17] Wang X, Liu Z R and Zhao D M 2014 *J. Opt. Soc. Am. A* **31** 872
[18] Zheng H P, Chen R P and Ooi C H R 2013 *Lasers Eng.* **24** 345
[19] Keshavarz A and Honarasa G 2014 *Commun. Theor. Phys.* **61** 241
[20] Zhou G Q 2014 *J. Opt. Soc. Am. A* **31** 1239
[21] Rui F, Zhang D W, Ting M, Gao X M and Zhuang S L 2013 *Optik* **124** 2969
[22] Miao Y, Wang G X, Zhan Q F, Sui G R, Zhang R F, Lu X M and Gao X M 2017 *Optik* **128** 201
[23] Qu Q L, Lu X M, Peng J and Su W X 2017 *Optik* **129** 50
[24] Zeng X Y, Miao Y, Wang G X, Zhan Q F, Hong R J and Zhang R F 2017 *Optik* **130** 481
[25] Torre A 2016 *Appl. Phys. B* **122** 55
[26] Ni Y Z and Zhou G 2013 *Opt. Commun.* **291** 19
[27] Ni Y Z and Zhou G 2012 *Appl. Phys. B* **108** 883
[28] Zhou G Q and Ru G Y 2013 *PIER* **143** 143
[29] Zhou G Q, Ji Z Y and Ru G Y 2016 *Laser Phys.* **26** 075002
[30] Sztul H I and Alfano R R 2006 *Opt. Lett.* **31** 999
[31] Guo C S, Yue S J and Wei G X 2009 *Appl. Phys. Lett.* **94** 231104
[32] Tao H, Liu Y X, Chen Z Y and Pu J X 2012 *Appl. Phys. B* **106** 927
[33] Liu Y X, Sun S H, Pu J X and Lü B D 2013 *Opt. Laser Technol.* **45** 473
[34] Lyubomir S, Suzana T, Ivan S, Ljiljana J and Alexander D 2015 *Opt. Commun.* **350** 301
[35] Collins S A 1970 *J. Opt. Soc. Am.* **60** 1168
[36] Schmidt P P 1976 *J. Phys. B: At. Mol. Opt. Phys.* **9** 2331
[37] Wen J J and Breazeale M A 1990 *Computational Acoustics* (Lee D, Cakmak A and Vichnevetsky R, Ed.) (New York: Elsevier)
[38] Gradshteyn I S and Ryzhik I M 1980 *Table of Integrals, Series, and Products* (New York: Academic Press)
[39] Gao C Q, Wei G H and Webe H 2000 *Sci. China Ser. A-Math.* **43** 1306
[40] Torner L and Torres J P 2005 *Opt. Express* **13** 873
[41] Ni Y Z and Zhou G Q 2015 *Lasers in Eng.* **30** 73
[42] Zhou G Q and Ru G Y 2015 *Lasers in Eng.* **30** 159
[43] Zhou G Q and Ru G Y 2013 *PIER* **141** 751
[44] Wang L, Zhao S M, Gong L Y and Cheng W W 2015 *Chin. Phys. B* **24** 120307
[45] Zou L, Wang L, Zhao S M and Chen H W 2016 *Chin. Phys. B* **25** 114215